Final Draft
of the original manuscript:

Wieland, D.C.F.; Degen, P.; Paulus, M.; Schroer, M.A.; Bieder, S.; Sahle, C.J.; Moeller, J.; Leick, S.; Chen, Z.; Struth, B.; Rehage, H.; Tolan, M..:

Formation of iron containing aggregates at the liquidair interface

In: Colloids and Surfaces B (2013) Elsevier

DOI: 10.1016/j.colsurfb.2013.03.006

Formation of iron containing aggregates at the liquid-air interface

D.C. Florian Wieland[a,b], Patrick Degen[c], Michael Paulus[b], Martin A. Schroer[b,d], Steffen Bieder[b], Christoph J. Sahle[e,b], Johannes Möller[b], Sabine Leick[c], Zhao Chen[b], Bernd Struth[d], Heinz Rehage[c], Metin Tolan[b]

[a] *Helmholtz-Zentrum Geesthacht, Max-Planck Straße 1, 21502 Geestacht, Germany*
[b] *Fakultät Physik / DELTA, 44221 Dortmund, Germany*
[c] *Fakultät Chemie, Physikalische Chemie II, Otto-Hahn-Straße 6, 44227 Dortmund, Germany*
[d] *Deutsches Elektronen Synchrotron (HASYLAB), Notkestraße 85, 22607 Hamburg, Germany*
[e] *Department of Physics, University of Helsinki, Helsinki, Finland*

Abstract

The early stages of the formation of inorganic aggregates, composed of iron compounds at the solution-air interface, were investigated in situ. The properties of the solution-air interface were changed by using different Langmuir layers. In order to get insight into the evolution of the sample system in situ, the processes were studied by x-ray scattering and spectroscopy techniques. The formation of aggregates was detected under cationic as well as under anionic Langmuir layers. The observed compounds lack long range order which indicates the formation of amorphous structures. This is supported by extended x-ray absorption fine structure measurements showing only minor order in the formed aggregates.

Keywords: interface, Langmuir films, aggregation

1. Introduction

The formation of inorganic structures in living organisms is a highly complex process for which an extremely high level of control is essential.[1] Nature utilizes a wide range of mineral polytypes and morphologies in the growth process which are chosen with respect to specific needs and functions.[2] The degree of perfection reached by living organisms is realized by a complex interplay of different physical, chemical, and biological functions which

Email address: florian.wieland@hzg.de (D.C. Florian Wieland)

were developed in a long evolutionary process. Up to now, only a fraction of these complex mechanisms is understood. The formation process is, for instance, controlled by macromolecules directing the type of the crystal, whereas the orientation of the crystal is affected by the interaction with interfaces.[3, 4, 5, 6] Thus, for the understanding of such growth processes and the transfer of growth principles, the influence of interfaces on the nucleation mechanism is crucial.

A large body of work has already been done in the field of nucleation processes occurring at interfaces. Here, aspects such as stereo-chemical matching or epitaxial growth were discussed as control mechanisms.[7, 8, 9, 10, 11] Recent studies indicate that a mineralization route, which passes through an amorphous precursor phase, is favored.[12, 13, 3, 14, 15, 16, 17] These observations are in agreement with molecular dynamics simulations which show that the type of crystal formed depends solely on the surface charge density.[18]

However, most of the cited works suffer from the drawback of being performed ex situ. Removing the samples from the aqueous environment may result in structural modifications. Therefore, in situ measurements investigating directly the interfacial structure are essential to establish a reliable picture of the events which occur at the liquid-air interface.

Due to their potential application, particles made of iron oxides such as magnetite (Fe_3O_4) or maghemite (γ-Fe_2O_3) are in the focus of current research.[19, 20, 21, 22, 23, 24] Here, nature also offers interesting applications such as the avian magnetometer system of birds [25], the magnetosomes of bacteria[26, 27, 28, 29, 30, 31], or the teeth in the radula of chiton. However, the production of single phase iron oxides in a liquid environment is rather difficult because a large variety of different structures, including oxides and hydroxides, can be formed.

Experiments investigating the formation process of iron containing compounds by the Langmuir-Blodgett technique show the formation of magnetite under Langmuir layers of 1-octadecanol using an using a iron(II) chloride solution.[32] The same study investigated monolayers of octadecyl amine, and no scattering signal from crystalline material was detected. Investigations of the adsorption process of nanoparticles and proteins at Langmuir monolayers show a strong dependence on the electrostatic interaction.[33, 34] Adsorption only occurs if the Langmuir layer has opposite charge than the adsorbant. Thus, for solutions containing iron ions it is reasonable that anionic Langmuir layers aid the growth of inorganic structures by lowering the barrier for

a heterogeneous nucleation. In contradiction to this, the work performed by Maas et al.[35] the growth of thin films of iron oxide at Langmuir layers with varying polarity (1- octadecanol, octadecanoic acid, octadecyl amine) could be observed by scanning electron microscopy. This study could not resolve the initial formation process. Also, structural information on the employed Langmuir layers were not accessible. An in situ study, performed on the absorption behavior of iron(III) at a Langmuir monolayer with a carboxylate headgroup, suggests covalent bonding of different complexes.[36, 37]

In this work, the aggregation process of iron compounds below lipid membranes was investigated in situ by means of x-ray reflectivity (XRR), grazing incidence diffraction (GID), and x-ray absorption fine structure (XAFS) spectroscopy. Amphiphilic molecules with different composition were used as nucleation sites in order to reveal the effect of a modified surface on the formation process. The selection of the amphiphiles was made on the basis of ex situ studies showing the aggregation at the interface.[35, 32] The structural integrity of the lipid film as well as the initial layer formation below the film were analyzed. With GID measurements the two-dimensional crystalline structure of the Langmuir film during the adsorption process was monitored. Furthermore, the formation of crystalline material at the interface can be detected. Complementary, XAFS experiments give information on the local ordering also for non crystalline materials.

In the presented sample system, low concentrated iron(III) chloride solutions were employed. By using higher concentrations, the fast formation process prohibited the observation of the initial stages. At the used concentrations an acceptable supersaturation level for the formation of iron containing compounds in the bulk volume can not be achieved. This problem was encountered by lowering the solubility product of the iron species by changing the pH value. To achieve this, ammonia was added to the atmosphere above the sample surface. Ammonia subsequently diffused into the sample's interface, thus raising the pH value and lowering the solubility product. Due to possible phase transformations, which depend on the chemical environment, other polymorphs, e.g. Fe_2O_3 or Fe_3O_4, can be formed.[38, 39]

2. Experimental details

X-ray reflectivity (XRR) measurements are sensitive to the laterally averaged electron density of the sample perpendicular to the surface and, thus, provides information of the layer structure.[40] The reflectivity $R(q_z)$ is given

in the kinematical approximation by

$$R(q_z) = R_{\mathrm{F}}(q_z)\Big|\frac{1}{\rho_s}\int\Big(\frac{d\rho(z)}{dz}\Big)\exp(iq_z\cdot z)dz\Big|^2 \quad (1)$$

with the electron density profile $\rho(z)$, the electron density of the substrate ρ_s, and the Fresnel reflectivity R_{F}.[41, 42]

Grazing incidence diffraction (GID) measurements yield information about the ordered lateral structure of the sample.[43] The x-ray beam impinges on the surface under a shallow angle, which is below the critical angle of total external reflection. Thus, the scattered intensity originates predominantly from the surface regime because the x-rays enter only a few nanometers into the sample.[44] The intensity is monitored as a function of the wave vector transfer $q_{||}$ parallel to the sample surface.[43, 45]

In an x-ray absorption spectroscopy (XAS) experiment the modulation of the absorption coefficient μ across an absorption edge of a specific element is monitored as a function of energy.[46] The absorption coefficient is modulated by the chemical environment of the element under investigation and information from the local structure around the absorbing atom up to a maximum distance of appropriate 10 Å can be gained.[46] The structure in the vicinity of the absorption edge is called the x-ray absorption near edge structure (XANES) and provides information on the local electronic and chemical structure. If the edge is investigated at much higher energies, the region is called extended x-ray absorption fine structure (EXAFS), which is determined mainly by the local structure around the investigated atom. By analyzing the EXAFS signal, information on e.g. the structure of the coordination shells surrounding the adsorbing atom can be obtained.

2.1. Sample preparation and measurements

Octadecanoic acid (purity $\geq$ 97%, AppliChem), 1,2-dipalmitoyl-sn-glycero-3-ethylphosphocholine (EPC) (purity $\geq$ 99%, Avanti Polar Lipids), 1,2-dipalmitoyl-sn-glycero-3-phosphocholine (DPPC) (purity $\geq$ 97%, Sigma) and 1-octadecanol (purity $\geq$ 96%, Merk) were used. Subphases of iron(III) chloride (purity $\geq$ 98%, Merck) were prepared with a concentration of 1 mmol/L and 100 mmol/L using ultra pure water (specific resistance 18.2 MΩcm). Due to the acid character of iron(III) chloride, the solution with a concentration of 1 mmol/L had a pH value of 3.02 and the solution with a concentration of 100 mmol/L of 1.48.

Langmuir films were prepared by spreading the lipid containing chloroform solution drop wise onto the subphase. After 20 minutes for evaporation of chloroform, the films were compressed to different surface pressures Π, which were kept constant during the measurements (Π = 10 mN/m, Π = 20 mN/m, and Π = 40 mN/m). In order to check whether the observed structural changes at the liquid surface are induced by the aggregation of iron compounds or by the interaction of ammonia with the amphiphilic molecules, reference measurements of Langmuir films on a pure water subphase in the presence of ammonia were conducted. After sample preparation the initial state of the system was characterized by XRR and GID measurements. Then ammonia was added to trigger the aggregation. The evolution of the sample system was monitored by alternatingly performed XRR and GID measurements.

The experiments were performed at beamline BW1 of DORIS III at DESY, Hamburg, Germany [47], using the liquid surface diffractometer and a photon energy of E = 9.5 keV. For the GID measurements an incident angle of 0.1° was chosen. The used custom made Langmuir trough was placed in a helium flushed chamber in order to suppress air scattering. The Langmuir trough was translated horizontally in order to reduce radiation damage. A similar set-up was used at beamline ID10B of the European Synchrotron Radiation Facility (ESRF), Grenoble, France (E = 22 keV).[48] Additional XRR measurements were performed with a Bruker AXS D8 advanced laboratory diffractometer (E = 8 keV).

XAFS experiments at the iron K-edge were performed at beamline BL8 of DELTA, Dortmund, Germany and beamline A1 of DORIS III at DESY, Hamburg, Germany.[49, 50] The incoming x-ray beam was tilted towards the sample resulting in an incident angle of 0.1°. By this, surface sensitivity was achieved.

The important changes within the reflectivity curves which indicate the formation of inorganic compounds at the interface appear at q_z lower than 0.2 Å^{-1}. Here, the statistical error in the data is not higher than 1 % . For the diffraction data, the statistical error for one data point was not higher than 5 %. In the x-ray absorption experiments the statistical error for a data point is not higher than 3 % . However, the main uncertainty of the results originate from the complexity of the investigated systems. Thus, in order to check the reproducibility of the results, each sample system was prepared several times.

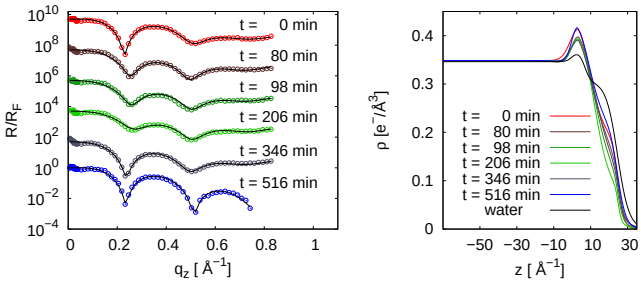

Figure 1: Left: Fresnel normalized reflectivities of an octadecanoic acid film (Π = 10 mN/m) at different times deposited on an iron(III) chloride solution. After a time of t = 75 min ammonia was added. The curves are shifted vertically for clarity. Right: Electron densities obtained by the refinement of x-ray reflectivity data.

3. Results and discussion

In order to check the influence of ammonia on the Langmuir monolayers, reference measurements were performed on pure water. These measurements were conducted at a surface pressure of Π = 20 mN/m. The concentration of ammonia in the helium atmosphere was tested by diffusion tubes (ISO 9001 purchased from Dräger) yielding a maximum concentration of 100 ppm during the experiments.

The analysis of the XRR data shows minor changes in the vertical density profiles (see in supporting information (SI) the reflectivity data in figure 1 and the resulting electron density profiles in figure 2).

The GID measurements confirm that ammonia has only a destabilizing effect on the lateral structure of the Langmuir layers (see SI). The Langmuir films of DPPC and 1-octadecanol show a decrease of their scattering amplitude accompanied by an increase of the width of the Bragg reflection indicating a shrinking of the crystalline patch size in the illuminated area. The XRR and GID data show that neither strong damage by ammonia to the monolayer nor beam damage can be observed.

The iron compounds, which are present in solutions, can vary significantly depending on the solution condition. The Fe^{3+} ion has a sixfold coordination accompanied by a strong tendency for hydrolysation in aqueous solutions. Due to this, a variety of different iron species e.g. $(Fe(OH)_{3-y})$, y $\neq$ 4 or chloro-complexes like $[FeCl(H_2O)_5]^{2+}$ can be found.[51, 52, 53, 54, 55] In the pH regime of our experiments, the soluble complexes $Fe(OH)^{+2}$ and $Fe(OH)_2^+$ dominate.[51]

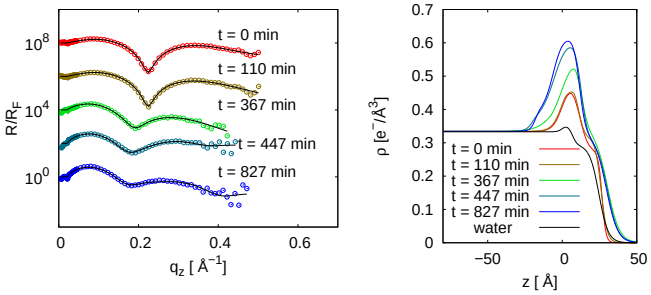

Figure 2: Left: Fresnel normalized reflectivities of an octadecanoic acid film ($\Pi = 20$ mN/m) at different times deposited on an iron(III) chloride solution. After a time of t = 75 min ammonia was added. The curves are shifted for clarity. After the last scan shown in the figure, the sample was found to be stable. Right: Electron densities obtained by the refinement of x-ray reflectivity data.

In a first step, the influence of the surface pressure on the nucleation process is discussed. A Langmuir monolayer which consists of octadecanoic acid having an anionic headgroup was prepared on an iron(III) chloride solution with a concentration of 1 mmol/L and was compressed to a surface pressure of $\Pi = 10$ mN/m. Figure 1 shows the electron density profiles obtained from the reflectivity data. The refined profiles show an increase of the headgroup's electron density, which can be explained by an adsorption of single iron(III) complexes at the Langmuir film (see SI), however, no further increase of the electron density below the headgroup within 516 min can be observed. Only a disturbance of the tailgroup structure is visible.

The experiment was then repeated with an elevated surface pressure of 20 mN/m. The obtained reflectivities and electron density profiles are shown in figure 2. The profiles show an increase of the electron density, which can be attributed to an aggregation of iron compounds at the interface. The electron density of the headgroup structure increases strongly, which indicates a penetration of the iron compounds into the Langmuir layer. In the final state, the tailgroup structure is smeared out. Thus, an aggregation of iron compounds only occurs if the surface pressure is increased above a critical threshold.

Figure 3 shows the electron density profiles obtained by the refinement of the XRR data of an EPC monolayer, which possesses a cationic headgroup. The Langmuir layer was compressed to a surface pressure of $\Pi = 20$ mN/m. The data show that already in the first measurement an increase of the electron density can be observed. This layer has a thickness of 50 Å without the

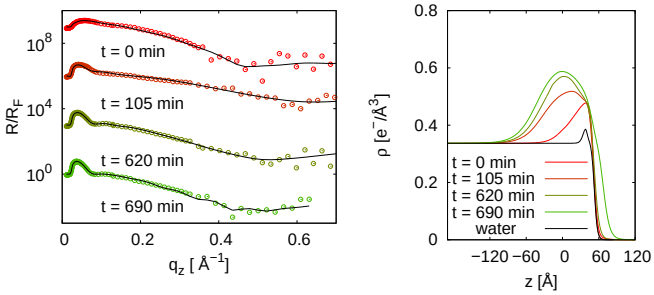

Figure 3: Left: Fresnel normalized reflectivities of an EPC film ($\Pi = 20$ mN/m) at different times deposited on an iron(III) chloride solution. After a time of t = 690 min ammonia was added. The curves are shifted for clarity. After the last scan shown in the figure, the sample was found to be stable. Right: Electron densities obtained by the refinement of x-ray reflectivity data.

addition of ammonia. The formation proceeds until a layer of 160 Å thickness was formed. After t = 690 min ammonia was added in order to check the saturation of the aggregation process. No further changes were observed. All density profiles do not reproduce the Langmuir layer's shape indicating a coalescence of the adsorbed material with the Langmuir layer.

In the case of 1-octadecanol, which has a non-ionic headgroup, an increase of the headgroup's electron density can be observed compared to the experiments on pure water , see figure 4.After ammonia was added, an further increase of the electron density at the interface can be observed. The electron density under the monolayer shows a plateau region at 0.44 e^- /Å^3 (see figure 4). The calculated electron density for a closed iron oxide (Fe_2O_3 layer is 2.6 e^- /Å^3 and for a closed layer of Lepidocrocite (FeOOH) is 1.23 e^- /Å^3. This indicates that no closed film is formed and only small aggregates accumulate at the interface.

In contrast, the system of a zwitterionic DPPC Langmuir layer (Π = 20 mN/m) deposited on an iron(III) chloride solution exhibits no formation process. Figure 5 shows the electron densities obtained from the XRR data. Only a disturbance of the monolayer structure is visible. For comparison, the electron density profile of DPPC on water is shown. The electron density of the DPPC layer in the presence of ammonia resembles the shape of the structure on pure water. This indicates that the forming iron species can not bind to the lipid headgroups in the presence of ammonia. This sample system was also investigated by compressing the DPPC layer to a surface pressure of $\Pi = 40$ mN/m (data not shown). The obtained electron density profiles show

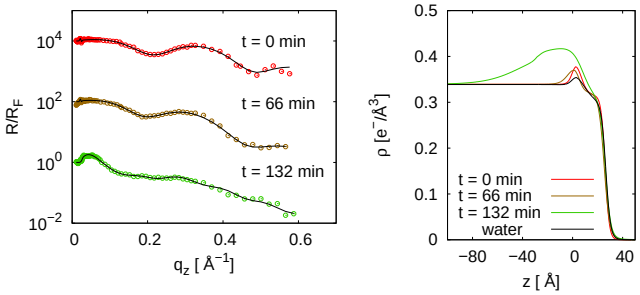

Figure 4: Left: Fresnel normalized reflectivities of an 1-octadecanol film (Π = 20 mN/m) at different times deposited on an iron(III) chloride solution. After a time of t = 60 min ammonia was added. The curves are shifted for clarity. After the last scan shown in the figure, the sample was found to be stable. Right: Electron densities obtained by the refinement of x-ray reflectivity data.

no aggregation of iron compounds. Accordingly, the zwitterionic layer seems to suppress the accumulation of aggregates at the interface but a precipitate could be observed after the experiment.

Figures 6 and 7 show the GID scans of selected samples. The Bragg rods are shown in the supporting information. In the case of the DPPC monolayer, where no mineralization occurs, the GID scan shows a change of the monolayer's tail tilt after the addition of ammonia (see figure 6). In the beginning, the Langmuir layer can be described by a hexagonal unit cell where the tails are in the upright position with a tilt angle of $\gamma = 0$ °. After ammonia is added, a transition to a rectangular unit cell occurs and the tilt angle of the tails increases to $\gamma = 28$ °. In the course of this change, the area per chain increases from 19.56 Å^2 to 22.30 Å^2. The full width of half maximum of the reflection at $q_{||}$= 1.508 Å^{-1} slightly decreases, which indicates an increasing size of the lateral patches from (339 Å $\pm$ 6Å) to (364 Å $\pm$ 7 Å). The state prior to the addition of ammonia differs from the state observed in the reference measurements on pure water. After ammonia is added, the DPPC Langmuir layer adopts the same state as in the reference measurements, which is also in accordance with literature.[56]

The lateral structure of the 1-octadecanol film shows only minor changes. The Langmuir layer can be described by a hexagonal unit cell and the position of the reflection is constant at $q_{||} = 1.520$ Å^{-1}, while only the intensity of the reflection decreases. This effect is caused by the ammonia (see reference measurements, SI).

For all systems only Bragg reflections from Langmuir layers are observable

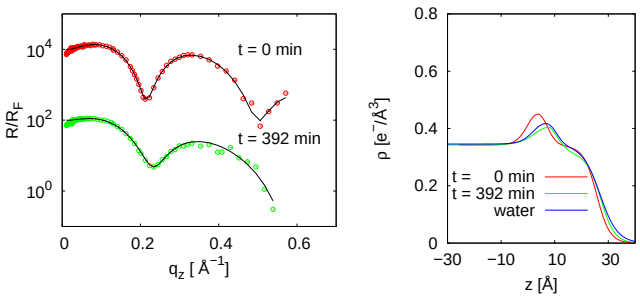

Figure 5: Left: Fresnel normalized reflectivities of a DPPC film (Π = 20 mN/m) at different times deposited on a subphase of iron(III) chloride solution. After a time of t = 64 min ammonia was added. The curves are shifted for clarity. After the last scan shown in the figure, the sample was found to be stable. Right: Electron densities obtained by the refinement of x-ray reflectivity data.

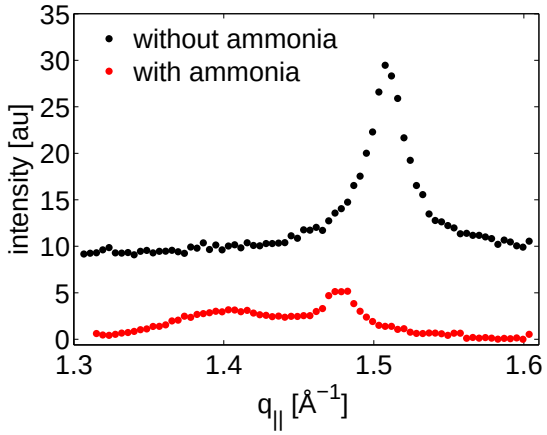

Figure 6: GID measurements of a DPPC monolayer on top of a iron(III) chloride solution. The surface pressure for all measurements was Π = 20 mN/m. Ammonia was added after a time of t = 50 min. In the beginning the Langmuir layer can be described by a hexagonal unit cell with a 6 fold degenerate diffraction peak at $q_{||} = 1.508$ Å^{-1}. In the presence of ammonia the lattice transforms to a rectangular unit cell where the diffraction peaks can be indexed as the degenerate (1,1) and (1,$\bar{1}$) at $q_{||} = 1.407$ Å^{-1} and the (0,2) diffraction peak can be ascribed to be at $q_{||} = 1.478$ Å^{-1}.

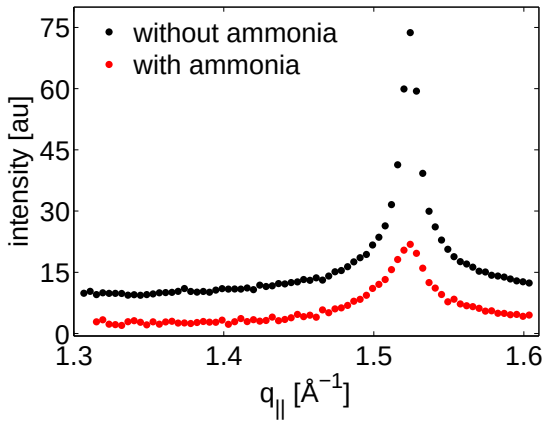

Figure 7: GID measurements of an 1-octadecanol monolayer on top of iron(III) chloride solution. The diffraction peak is at $q_{||} = 1.528$ Å^{-1}. The surface pressure was $\Pi = 20$ mN/m. Ammonia was added after a time of t = 60 min.

and none stemming from crystalline iron compounds, which indicates the formation of amorphous aggregates. A diffraction scan of the final state of the sample covering a larger q range is enclosed in the SI and shows only the reflection from the Langmuir layer. The decrease of the scattering intensity shows that the aggregation process advances simultaneously with the degeneration of the Langmuir films.

A Brewster angle microscopy (BAM) image obtained on iron(III) chloride solution under an octadecanoic acid monolayer is shown in figure 8. The image shows bright spots overlapping the reflected signal from the Langmuir layer. Due to the high intensity, the structures are assumed to be inorganic, which is consistent with the formation of iron aggregates at the interface.

As the material aggregated at the interfaces exhibits no long range order, which is indicated by the GID measurements, in situ surface sensitive XAFS experiments were conducted at the iron K-edge in order to collect information on the local ordering of the iron ions. XANES experiments on iron(III) chloride solutions with two different kinds of Langmuir layers and iron(III) chloride concentrations are shown in figure 9. The iron(III) chloride concentrations were 1 mmol/L and 100 mmol/L, respectively. Langmuir layers of octadecanoic acid and 1-octadecanol were used because both showed the formation of a layer with different structure.

By using octadecanoic acid monolayers on a subphase with a concentra-

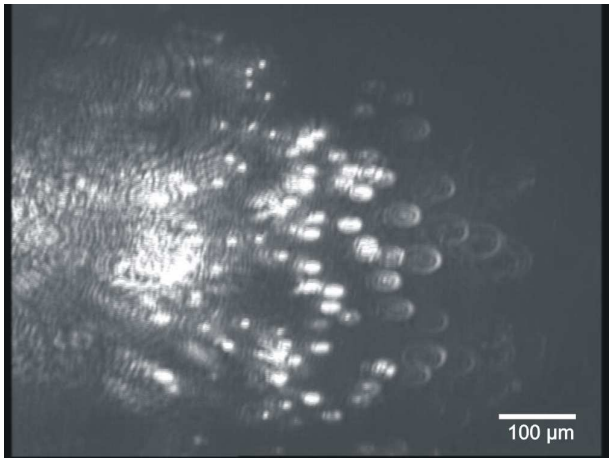

Figure 8: BAM image of an octadecanoic acid monolayer in an advanced state of the formation process.

tion of 1 mmol/L iron(III) chloride no changes in the structure of the absorption edge can be observed (see figure 9b filled symbols). This indicates that the formed layers, which are seen in the XRR experiments, exhibit no structural rearrangement. In the following the experiment was repeated using an increased subphase concentration of 100 mmol/L. These spectra are depicted in figure 9b (open symbols). A change in the near edge structure is visible. The intensity of the pre-edge at an energy of 7.11 keV increases, which is caused by a change of the iron coordination to a less centro-symmetric character.[53] The experiments performed on an 1-octadecanol monolayer and subphase concentrations of 1 mmol/L and 100 mmol/L are shown in figure 9a. No changes of the absorption edge can be observed after ammonia was added. From this data it can be concluded that only for octadecanoic acid in combination with a subphase concentration of 100 mmol/L a structural ordering can be detected.

In order to get access to the local structure of the aggregates, EXAFS scans were conducted on the sample systems of octadecanoic acid and, as a reference, on 1-octadecanol. Subphases with a concentration of 100 mmol/L of iron(III) chloride were used. The $\chi(k)$ is shown in the supporting information. The Fourier transformed EXAFS signals χ(R), which provide information on the coordination shells surrounding the absorbing atom, are shown in figure 10. For the experiments utilizing the 1-octadecanol monolayer, no changes of the local environment around the absorbing iron atom atom can

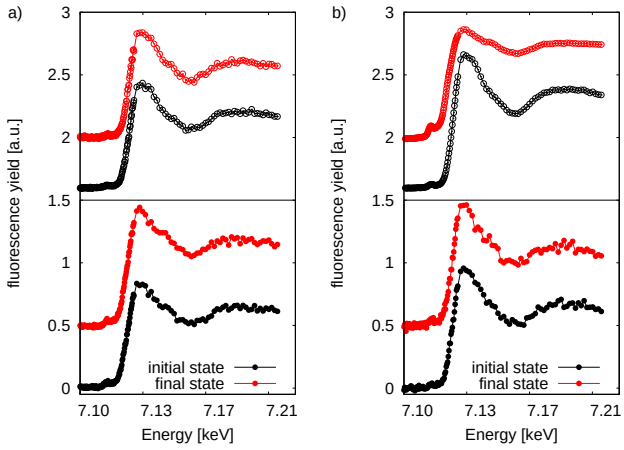

Figure 9: XANES measurements on iron(III) chloride solutions and different Langmuir layers. Filled symbols represent a concentration of 1 mmol/L and open symbols a concentration of 100 mmol/L. a) 1-Octadecanol. b) Octadecanoic acid.

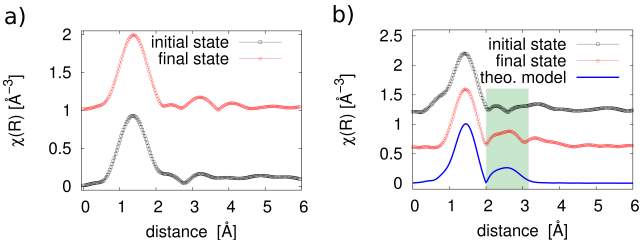

Figure 10: Fourier transformed EXAFS data $\chi(R)$ obtained on samples of 100 mmol/L iron(III) chloride solution . a) 1-octadecanol. b) octadecanoic acid.

be found, in agreement with the XANES experiments. The χ(R) shows only one coordination shell around the iron atom, which can be attributed to a reasonable oxygen-iron coordination.

In contrast, the sample with the octadecanoic acid present at the interface shows the formation of a further coordination shell visible by a second maximum in the χ(R). This indicates an increased order around the iron atoms. Qualitative information about the coordination shells were extracted by fitting the χ(R) using the program package Artemis.[57] This analysis shows a minor iron content in the second coordination shell of 2 ± 1 iron atoms on average. For comparison, in the hematite structure five iron atoms are present in the second coordination shell.

4. Conclusion

XRR measurements revealed the formation of iron compounds at different Langmuir layers. The aggregation is inhibited only at the interface of the zwitterionic DPPC. This is in contrast to the studies of Sarkar et al.[58], which report on the formation of nanoparticles at DPPC monolayers even without ammonia. However, the concentrations and the surface pressures differ to our study which may explain the discrepancy. On the other hand, in the mentioned study the aggregation is only observed indirectly by the variation of the surface pressure and ex situ TEM images which are no evidence for a particle formation at the interface in situ.

The changes in the DPPC Langmuir layer can be explained by a binding of iron complexes to the headgroup as observed by Wang et al.[36] By the addition of ammonia, the iron compounds are removed from the headgroup structure and the DPPC layer adopts the same structure as on a pure water subphase. Similar changes were observed by using divalent ions where a closer arrangement of the lipids could be observed due to a binding of Zn^{2+} to the phosphate moiety inducing a conformational change.[59] However, this effect was not as strong as for our samples.

In the case of Langmuir layers with cationic, anionic and non-ionic headgroups an aggregation at the interface was observed. The XRR experiments show the penetration of the Langmuir layer by the compounds. It can be excluded by the XRR measurements that a closed film is formed under the monolayers. It is more likely that small aggregates nucleate at the liquid-air interface. This conclusion is supported by BAM images from the water-air interface showing the formation of isolated inorganic aggregates. Indicators for such a behavior were also observed by other optical ex situ studies.[35]

As our experiments were performed at a pH value lower 3, the carboxylate headgroup of octadecanoic acid will not be dissociated as the pK_a value is 5.3. However, this does not exclude the binding of ions or complexes to the headgroup as this depends on the pH value and ion concentration.[60]

The GID measurements show a stable Langmuir layer during the mineralization process. In all measurements no diffraction signals from crystalline iron oxides were observed. This may indicate the formation of amorphous material since even small aggregates would give rise to a GID signal.

The surface sensitive XAFS measurements show that the layers formed by using subphases of iron(III) chloride with a concentration of 1 mmol/L are amorphous and lack long range order, which is in agreement with the

GID experiments. By increasing the iron(III) chloride concentration to 100 mmol/L, the layers formed under octadecanoic acid begin to develop a certain order, which highlights the influence of a cationic headgroup on the formation process.

The observation made by the XAFS and XRR experiments indicate a differing nucleation mechanism at the Langmuir layers depending on the type of headgroup. The structure of the non ionic and anionic formed layers differ significantly from the layers formed at the cationic headgroup. Furthermore, the XAFS experiments show that, at the anionic headgroup, inorganic compounds with an increased local order around the iron atoms exist.

The presented XRR data shows that already at the beginning the headgroups of the Langmuir layers exhibit an increased electron density which can be explained by an adsorption of iron species right at the beginning. This was also observed in a study by Wang et al.[36, 61] investigating the interaction of iron(III) with carboxylate headgroups. Iron species bind to the Langmuir layers acting as seed layer. Upon the addition of ammonia, the pH value in the interface region changes, which leads to a further aggregation of iron compounds. It could be observed that the nucleation only occurs if the surface pressure of the Langmuir layer has reached a critical point. This shows that a sufficient density of the Langmuir layer must be achieved for a successful layer formation. The structure of the forming layer can be influenced by the headgroup of the Langmuir film present at the interface. By using carboxylate headgroups, an ordering in the iron oxide layer can be achieved, which is absent when using non ionic headgroups.

In summary, we observed the aggregation of amorphous iron compounds under different monolayers. The data shows that a model, which explains the aggregation by simple electrostatic forces between the positively charged iron ions and differently charged head groups resulting in an accumulation or depletion of ions at the interface, cannot explain our observations, because aggregates were observed at anionic, cationic and non-ionic Langmuir layers. Only in the case of the zwitterionic DPPC no formation was observed. The local order inside the amorphous aggregates could be influenced by changing headgroups but is still not as high as in crystalline material.

acknowledgements

We acknowledge the ESRF and HASYLAB (DESY) for providing synchrotron radiation. We also acknowledge Alexei Vorboiev (ID10B) for tech-

nical support during the beamtimes. D.C.F.W. and C.Z. thank the NRW Forschungsschule "Forschung mit Synchrotronstrahlung in den Nano- und Biowissenschaften" for financial support. M.A.S. and S.B. acknowledge the BMBF contract No. 05K10PEC for funding. For his work during the ESRF beamtime we thank Jens Beneken. Ch.S. is supported by the Academy of Finland (No. 1256211) and the University of Helsinki Research Funds (No. 490076).

References

[1] H. Lowenstam, S. Weiner, On Biomineralization, Oxford University Press, Oxford, 1989.

[2] F. Meldrum, Inter. Mater. Rev. 48 (2003) 187.

[3] A. Xu, Y. Ma, H. Coelfen, J. Mater Chem. 17 (2007) 415.

[4] N. Sommerdijk, G. de With, Chem. Rev. 108 (2008) 4499.

[5] S. Mann, D. Archribald, J. Didymus, T. Douglas, B. Heywood, F. Meldrum, N. Reeves, Science 261 (1993) 1286.

[6] S. Wiener, Crit. Rev. Biochem. 20 (1986) 365.

[7] K. K. Sand, M. Yang, E. Makovicky, D. J. Cooke, T. Hassenkam, K. Bechgaard, S. L. S. Stipp, Langmuir 26 (2010) 15239.

[8] S. Mann, B. Heywood, S. Rajam, J. Birchall, Nature 334 (1988) 692.

[9] S. Mann, Biomineralisation; Principles and Concepts in Bioinorganic Materials Chemistry, Oxford University Press, Oxford, 2001.

[10] S. Mann, Biomimetic Materials Chemistry, VCH, Weinheim, 1996.

[11] E. DiMasi, V. Patel, M. Sivakumar, M. Olszta, Y. Yang, L. Gower, Langmuir 18 (2002) 8902.

[12] B. P. Pichon, P. H. H. Bomans, P. M. Frederik, N. A. J. M. Sommerdijk, J.Am. Chem. Soc. 130 (2008) 4034.

[13] E. M. Pouget, P. H. H. Bomans, A. Dey, P. M. Frederik, G. de With, N. A. J. M. Sommerdijk, J.Am. Chem. Soc. 132 (2010) 11560.

[14] M. Fricke, D. Volkmer, Crystallization of calciumm carbonate beneath insoluble monolayers: suitable models of mineral-matrix interactions in biomineralization, in N. Kensuke, Biomineralization II, Springer-Verlag, Berlin/Heidelberg, 2007.

[15] E. DiMasi, M. Olszta, V. Patel, L. Gowe, Cryst. Eng. Comm. 5 (2003) 346.

[16] C. L. Freeman, J. H. Harding, D. M. Duffy, Langmuir 24 (2008) 9607.

[17] G. K. Hunter, J. O'Young, B. Grohe, M. Karttunen, H. A. Goldberg, Langmuir 26 (2010) 18639.

[18] G. A. Tribello, F. Bruneval, C. Liew, M. Parrinello, Journal of Physical Chemistry B 113 (2009) 11680.

[19] K. S. Patil, V.and Mayya, S. Pradhan, M. Sastry, J. Am. Chem. Soc. 119 (2009) 9281.

[20] B. Berkovskyl, V. Bashtovoy, Magnetic Fluids and Applications Handbook, Begell House, New York, 1996.

[21] A. K. Gupta, M. Gupta, Biomaterials 26 (2005) 3995.

[22] Q. Pankhurst, J. Connolly, S. Jones, J. J. Dobson, Appl. Phys. 36 (2003) 167.

[23] M. Brust, C. Kiely, Colloids Surf. 202 (2002) 175.

[24] P. Degen, D. Wieland, M. Paulus, M. Schroer, M. Tolan, H. Rehage, Colloid Poly. Sci. 291 (2013) 653.

[25] G. Falkenberg, G. Fleissner, K. Schuchardt, M. Kuehbacher, P. Thalau, H. Mouritsen, D. Heyers, G. Wellenreuther, G. Fleissner, PLoS ONE 5 (2010) 9231.

[26] J. Miot, K. Benzerara, G. Morin, A. Kappler, M. Obst, G. E. Brown, Jr., F. Guyot, Acta 73 (2009) A884.

[27] D. Archibald, S. Mann, Nature 364 (1993) 430.

[28] S. Mann, J. Hannington, R. Williams, Nature 324 (1986) 565.

[29] V. Wade, S. Levi, P. Arosio, A. Treffry, P. Harrison, S. Mann, J. Mol. Biol. 221 (1991) 1443.

[30] L. Addadi, S. Weiner, Angew. Chem. Int. Ed. 31 (1992) 153.

[31] F. Meldrum, B. Heywood, S. Mann, Science 257 (1992) 522.

[32] H. Lin, J. Cryst. Growth 192 (1998) 250.

[33] P. Degen, M. Paulus, M. Maas, R. Kahner, S. Schmacke, B. Struth, M. Tolan, H. Rehage, Langmuir 24 (2008) 12958.

[34] S. Tiemeyer, M. Paulus, M. Tolan, Langmuir 26 (2010) 14064.

[35] M. Maas, P. Degen, H. Rehage, H. Nebel, M. Epple, Colloid Surface A 354 (2010) 149.

[36] W. Wang, R. Y. Park, A. Travesset, D. Vaknin, Phys. Rev. Lett. 106 (2011) 56102.

[37] W. Wang, R. Park, D. Meyer, A. Travesset, D. Vaknin, Langmuir 27 (2011) 11917.

[38] D. Fu, P. G. Keech, X. Sun, J. C. Wren, Phys. Chem. Chem. Phys. 13 (2011) 18523.

[39] U. Schwertmann, R. Cornell, Ironoxides in the Laboratory, VCH Publischers, New York, 2001.

[40] S. Sinha, E. Sirota, S. Garoff, H. Stanley, Phys. Rev. B 38 (1988) 2297.

[41] M. Tolan, X-ray Scattering from Soft-matter thin Films - Material Science and Basic Research, Springer Tracts in Modern Physics 148, Springer, Berlin, 1999.

[42] B. Ocko, X. Wu, E. Sirota, S. Sinha, M. D., Phys. Rev. Lett. 72 (1994) 242.

[43] K. Kjaer, Physica B 198 (1994) 100.

[44] H. Dosch, Phys. Rev. B. 35 (1987) 2137.

[45] J. Als-Nielsen, K. Kjaer, X-ray reflectivity and diffraction studies of liquid surfaces and surfactant monolayers, Vol. 211 of The proceedings of the Nato Advanced Study Institute, Phase transitions in soft condensed Matter, Plenum Press, 1989.

[46] D. Koningsberger, R. Prins (Eds.), X-ray absorption -Principles, Applications, Techniques of EXAFS, SEXAFS and XANES, John Wiley and Sons, New York, 1988.

[47] R. Frahm, J. Weigelt, G. Meyer, G. Materlik, Rev. Sci. Instrum. 66 (1995) 1677.

[48] D. Smilgies, N. Boudet, B. Struth, O. Konovalov, J. Synchroton Radiat. 12 (2005) 329.

[49] D. Luetzenkirchen-Hecht, R. Wagner, U. Haake, A. Watenphul, R. Frahm, J. Synchrotron Radiat. 16 (2009) 264.

[50] E. Welter, AIP Conf. Proc. 1234 (2009) 955.

[51] A. Stefansson, Environ. Sci. Technol. 41 (2007) 6117.

[52] R. Byrne, Y. Luo, R. Young, Mar. Chem. 70 (2000) 23.

[53] W. Liu, B. Etschmann, J. Brugger, L. Spiccia, G. Foran, B. McInnes, Chem. Geol. 231 (2006) 326.

[54] B. Tagirov, I. Diakonov, O. Devina, A. Zotov, Chem. Geol. 162 (2000) 193.

[55] F. Millero, W. Yao, J. Aicher, Mar. Chem. 50 (1995) 21.

[56] I. Estrela-Lopis, G. Brezesinski, H. Möhwald, Chem. Phys. Lipids 131 (2004) 71.

[57] B. Ravel, M. Newville, J. Synchrotron Radiat. 12 (2005) 5371.

[58] R. Sarkar, P. Pal, M. Mahato, T. Kamilya, A. Chaudhuri, G. B. Talapatra, Colloid Surface B 79 (2010) 384.

[59] S. Kewalramani, H. Hlaing, B. M. Ocko, I. Kuzmenko, M. Fukuto, J. Phys. Chem. Lett. 1 (2010) 489.

[60] S. Cantin, S. Peralta, P. Fontaine, M. Goldmann, F. Perrot, Langmuir 26 (2010) 830.

[61] W. Wang, J. Pleasants, R. Park, I. Kuzmnko, D. Vaknin, J. Colloid. Interf. Sci. 384 (2012) 45.